

The Response of Tropical Climate to the Equatorial Emergence of Spiciness Anomalies*

NIKLAS SCHNEIDER

International Pacific Research Center, and Department of Oceanography, University of Hawaii at Manoa, Honolulu, Hawaii

(Manuscript received 28 January 2003, in final form 29 August 2003)

ABSTRACT

The ocean–atmosphere response to the surfacing of temperature anomalies from the oceanic thermocline is a key process in climate variability with decadal time scales. Using a coupled general circulation model, it is shown how density-compensating temperature and salinity (spiciness) anomalies emerging in the upwelling region of the equatorial Pacific modulate tropical climate.

Upon reaching the surface in the central equatorial Pacific, warm and salty spiciness anomalies increase sea surface temperature and salinity, and vent their heat anomaly to the atmosphere, primarily by the latent heat flux. The associated surface buoyancy flux increases vertical mixing, and thereby dampens surface temperature anomalies. The moisture added to the atmosphere increases precipitation in the western Pacific and intertropical convergence zone, and strengthens the trade winds east, and weakens them west of the date line. Central equatorial Pacific surface temperatures are slightly warmed by the resulting deepened thermocline, and additional warm spiciness anomalies due to a northward displacement of the climatological spiciness front on the equator, recycling salt anomalies in the shallow equatorial circulation and subduction from the Southern Hemisphere. From the Northern Hemisphere source regions of equatorial thermocline waters, cool and fresh anomalies result from the increased air–sea freshwater fluxes and wind-driven changes of the flow paths in the thermocline. The amplitudes of the model's El Niño–La Niña are diminished by warm spiciness anomalies due to a reduction of the temperature gradient in density coordinates that controls the thermocline feedback.

The coupled response is qualitatively consistent with a coupled climate mode that results from a positive feedback between the equatorial emergence of spiciness anomalies and the equatorial pycnocline and Southern Hemisphere responses, and a delayed, negative feedback due to Northern Hemisphere subduction. However, feedbacks are weak, and, at best, slightly enhance a decadal modulation of the Tropics due to spiciness anomalies generated by stochastic atmospheric forcing.

1. Introduction

In the tropical Pacific the atmospheric Hadley cell transports freshwater collected by evaporation in the subtropics to the low-latitude regions of deep atmospheric convection and precipitation. The ocean balances this freshwater transport by equatorward flow of salty waters in the thermocline. In the upwelling regions of the equatorial Pacific these waters return to the surface as part of a delicate, coupled ocean–atmosphere balance between winds, vertical deflections of isopycnals, and sea surface temperature. The salinity of the upwelled waters modulates this balance by its influence on ocean density, but lack of influence on the atmo-

sphere. This modulation is investigated here with a coupled ocean–atmosphere model.

A convenient description of the effect of ocean temperature and salinity on the coupled system is in terms of ocean density and spiciness. Density affects the ocean dynamics; its low-frequency adjustment is governed by wave dynamics. Spiciness describes the temperature and salinity of water of a given density, with hot and salty water having a high spiciness (Munk 1981). In the upper ocean, with an approximate constant equation of state, spiciness is a passive tracer. Upon surfacing, however, spiciness anomalies affect air–sea interaction due to their temperature signals.

As an example of this effect, compare the eastern tropical Pacific, where temperatures decrease with increasing density, with an isothermal ocean where density stratification results from an increase of salinity with depth. In such an ocean, changes of wind-driven upwelling neither affect SST nor feed back on the wind, in contrast to the eastern tropical Pacific where such feedbacks are essential. Far from being of academic interest only, this situation is realized in the western

* International Pacific Research Center Contribution Number 231 and School of Ocean and Earth Science and Technology Contribution Number 6249.

Corresponding author address: Dr. Niklas Schneider, International Pacific Research Center, University of Hawaii at Manoa, 1680 East West Road, Honolulu, HI 96822.
E-mail: nschneid@hawaii.edu

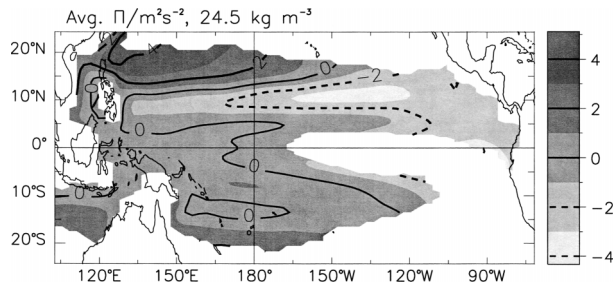


FIG. 1. Time-averaged Montgomery streamfunction on the $24.5\text{-}\sigma_{\theta}$ surface estimated from the average of all model experiments. The flow proceeds on the Northern (Southern) Hemisphere with a high streamfunction to the right (left). Contour interval is $2\text{ m}^2\text{ s}^{-2}$, with grayscale on the right.

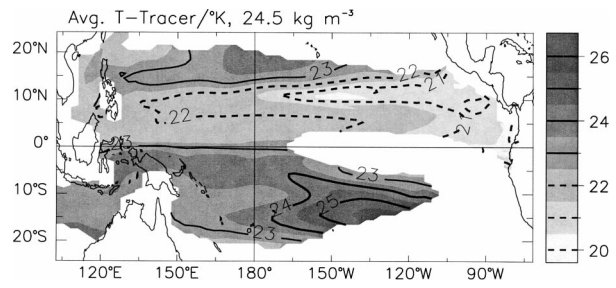


FIG. 2. Average temperature on the $24.5\text{-}\sigma_{\theta}$ isopycnal from the coupled model integration. Contour interval is 1 K, with grayscale on the right.

equatorial Pacific, where excess precipitation leads to a salt-stratified, near-isothermal layer with profound impacts on the response of SST to changes of winds (Lukas and Lindstrom 1991).

In the central and eastern Pacific, upwelling brings waters to the surface, whose spiciness results from conditions at midlatitude source regions and along transit paths in the oceanic thermocline. Low-frequency anomalies of the upwelling process have been hypothesized to cause decadal variations in the tropical climate. These perturbations can be initiated by changes of the upwelling rate, as part of changes of the shallow subtropical or equatorial cells (Kleeman et al. 1999), or by anomalies of the temperature of the upwelled waters (Gu and Philander 1997) due to an anomalous deep thermocline, or due to changes of temperature on isopycnals (Schneider 2000; Giese et al. 2002; Yeager and Large 2004). Only the last process fundamentally depends on ocean salinity or spiciness anomalies—the others are possible in an isohaline ocean.

The resulting adjustment of the ocean–atmosphere system is of interest here. Gu and Philander (1997) proposed that warm anomalies upwelling in the tropical Pacific modulate the amplitude and phase of ENSO and generate anomalies of opposite polarity at the subtropical source regions of thermocline waters. Schneider (2000) hypothesized that the emergence of warm anomalies at the western end of the equatorial cold tongue strengthens the equatorial trades and enhances upwelling. The off-equatorial wind response alters the advective paths on isopycnal surfaces, and, thereby, feeds back on the flux and spiciness of waters upwelling at the equator. Giese et al. (2002) suggested that SST perturbations due to the equatorial emergence of Southern Hemisphere, warm spiciness anomalies are amplified by air–sea interaction and account for the observed tropical climate shift to warmer conditions in 1976/77.

These conjectures are investigated here by studying the adjustment of the tropical climate to the equatorial emergence of spiciness anomalies using a perturbation experiment with a coupled ocean–atmosphere model. In the following, we discuss the coupled model, describe

the experiment and signal detection, and present the coupled responses in terms of the surface temperature and air–sea fluxes in the Tropics. We then turn to the question of whether the oceanic changes are consistent with a coupled climate mode. Next, changes of interannual anomalies in the Tropics, and those that result from atmospheric teleconnections to the midlatitudes, are presented. In the final section, conclusions will be summarized and discussed in light of decadal climate dynamics and model limitations.

2. Coupled model

The model, ECHO-2 (Frey et al. 1997), couples the European Centre/Hamburg atmospheric general circulation model and the Hamburg ocean primitive equation general circulation model. The ocean model has 20 levels in the vertical and a horizontal resolution of 2.8° in latitude and longitude in the midlatitudes. Toward the Tropics the resolution increases to 0.5° latitude to better represent the equatorial wave guide. The atmospheric component (ECHAM4) is a 19-level spectral model at a T42 trapezoidal resolution (Roeckner et al. 1996), with a full suite of subgrid-scale parameterizations. Within 60° latitude of the equator, the ocean and atmosphere exchange momentum, heat, and freshwater without flux correction. Poleward of 60° latitude, surface temperature and salinity are relaxed to observed climatologies.

The mean state, seasonal cycle, and interannual variability of the simulations are similar to observations (Frey et al. 1997; Pierce et al. 2000). Compared to its predecessors used in the studies of Latif and Barnett (1994) the model has much reduced tendencies to exacerbate the equatorial cold tongue and produce a double intertropical convergence zone.

In light of the importance of thermocline properties, we show the simulated Montgomery streamfunction (Fig. 1) and the temperature (Fig. 2) on the $24.5\text{-}\sigma_{\theta}$ surface in the upper thermocline. The flow on the isopycnal (Fig. 1) originates in the Northern and Southern Hemisphere outcrop regions and proceeds equatorward. In the Northern Hemisphere, Ekman pumping associated with the intertropical convergence zone forces waters onto a near-westward trajectory, and the majority

of the Northern Hemisphere waters approach the equator via the western boundary (see McCreary and Lu 1994). In contrast, Southern Hemisphere waters approach the equator primarily on direct, interior pathways.

The temperature on isopycnals reflects the gradients on the outcrops. In the Northern Hemisphere, waters are warm and salty off of Hawaii and along the transit to the western boundary, and are cool and fresh toward the equator. The equator is marked by a front to the warm and salty Southern Hemisphere. Water masses and flows in the thermocline are overall realistic compared to the observations (Johnson and McPhaden 1999), even though the simulated Indonesian throughflow consists primarily of waters of Southern Hemisphere origin (Schneider 2000), unlike observations that suggest a Northern Hemisphere origin (Gordon 1986).

The model's ENSO is characterized by temperature anomalies in the equatorial Pacific centered between 120° and 150°W of the order of 1–2 K, with a period of 2–3 yr. It evolves according to a delayed, damped oscillator: an SST anomaly in the equatorial cold tongue is reinforced by its interaction with the wind stress via the thermocline feedback. A cold SST anomaly in the equatorial cold tongue enhances the equatorial east–west temperature gradient and westward wind stress. This alters the east–west slope of the pycnocline, exposes deeper and cooler isopycnals to the surface, and reinforces the initial temperature tendencies. At the same time, off-equatorial Rossby waves are generated, which, after reflection off the western boundary, terminate the event.

3. Experiment

Because this work is motivated by decadal climate variability, we seek the coupled response to spiciness anomalies that emerge at the equator continually for several years and longer. To this end, density-compensated temperature and salinity (T – S) anomalies are introduced into the ocean thermocline, such that the circulation carries them to the equatorial outcrop regions.

Two experimental designs are considered: perturbations of the initial conditions and continual, in situ generation. As an initial value problem, spiciness anomalies have to be staged upstream of the equatorial upwelling regions such that emerging T – S perturbations are of approximately constant magnitude for the duration of the experiment, that is, for years to a decade. This requires knowledge of the advective path and mixing along the way, including changes due to the emerging spiciness perturbations, and intermingles two formidable problems: the propagation and attenuation of spiciness anomalies in the oceanic transit and the coupled response after their equatorial emergence. Therefore, the following approach is employed.

Spiciness perturbations are generated in the western equatorial Pacific thermocline by artificial, time-con-

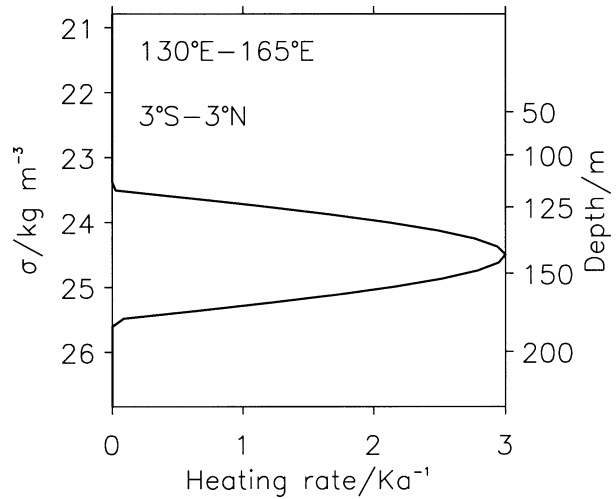


FIG. 3. Heating rate (K yr^{-1}) of waters as a function of density. Salinity is adjusted at every time step such that density is undisturbed. For reference the mean depth of isopycnals is denoted on the right axis. The forcing is applied on isopycnals in the upper thermocline in the area from 3°S to 3°N, and from 130° to 165°E. The heating occurs typically between 100 and 200 m.

stant sources of heat and freshwater. For potential densities $\sigma \in [\sigma_1, \sigma_2]$, the ocean is heated by

$$F(x, y, \sigma) = F_0(x, y) \sin\left(\frac{\pi}{2} \frac{\sigma - \sigma_1}{\sigma_2 - \sigma_1}\right), \quad (1)$$

where $F_0(x, y)$ is the forcing amplitude as a function of position, and salt is added such that the density of the water remains constant. Temperature and salinity are not perturbed on isopycnals outside of the density range $[\sigma_1, \sigma_2]$. The forcing is applied at every time step to temperature using the instantaneous density field. The corresponding salinity adjustment is then obtained from the model's equation of state.

The forcing is applied in the western Pacific from 3°S to 3°N, and from 130° to 165°E on isopycnals in the equatorial undercurrent, $\sigma_1 = 23.5 \text{ kg m}^{-3}$ and $\sigma_2 = 25.5 \text{ kg m}^{-3}$ (Fig. 3), typically at a depth between 100 and 200 m. This location upstream from the central and eastern Pacific equatorial emergence regions allows feedbacks in the location of equatorial outcrop of isopycnals without requiring exact knowledge of the propagation from subtropical latitudes. The density range ensures that the signal emerges in the central and eastern Pacific and coincides with the main decadal spiciness signal described by Schneider (2000). The amplitude of the forcing F_0 corresponds to a heating of 3 K yr^{-1} , required to heat water parcels passing through the forcing region by about 1 K.

Two experiments are performed—one with F_0 increasing the ocean's temperature and salinity (experiment 'WARM'), and one with the same amplitude cooling and freshening (experiment 'COOL'). Each experiment is run for 10 model years, and is repeated 3 times,

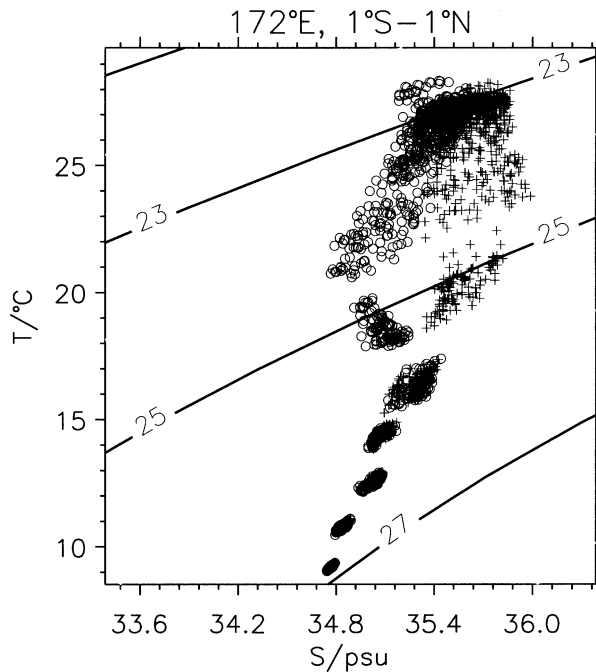


FIG. 4. Temperature-salinity diagram at 172°E between 1° latitude of the equator for the experiments with warm (plus symbols) and cool (circles) spiciness forcing. Shown are annual-averaged values for the last 9 yr of three realizations of each experiment. Contour lines depict potential density (kg m^{-3}).

with differences evolving due to truncation error of initial conditions and calculation. The coupled model is, thus, integrated for a total of 60 yr to estimate the response to the spiciness forcing and to distinguish it from internal variability of the coupled system.

The T - S diagram on the equator east of the forcing region (Fig. 4) shows the resulting perturbation of the spiciness: for σ , between 23.5 and 25.5 kg m^{-3} , the T - S traces are well separated with large spiciness anomalies of the order of 1–2 K.

4. Spiciness tracer and feedbacks

To distinguish the forced spiciness anomalies from changes of temperature and salinity due to the coupled response, a tracer χ is introduced in the ocean model, with dynamics and numerics that mimic those of temperature and salinity exactly. Initially it is zero everywhere, and forced by F in the same manner as temperature. At the surface, χ is removed by a relaxation to zero with a time scale of 100 days. In the thermocline, χ , therefore, measures the temperature perturbation associated with the spiciness forcing. The feedback of temperature in the thermocline is then estimated by the difference of the total temperature and the tracer concentration. Close to the surface this estimation of the feedback is problematic because the air-sea heat flux and tracer fluxes are similar, but not identical.

The feedback of temperature is split into signals due

to the adjustment of isopycnal depths, dT_ρ , and due to changes of temperature on isopycnals, dT_n . These are estimated from a coordinate transformation that converts changes of temperature dT and salinity dS to density and spiciness on isopycnal surfaces (Bindoff and McDougall 1994). Given dT , dS , the density change $d\rho = -\alpha dT + \beta dS$, and the background oceanic stratification T_0 , S_0 , and ρ_0 , the temperature anomalies dT_ρ and dT_n are determined by

$$\begin{aligned} dT &= \left. \frac{\partial T_0}{\partial \rho} \right|_{\rho_0} d\rho + dT_n \\ dS &= \left. \frac{\partial S_0}{\partial \rho} \right|_{\rho_0} d\rho + dS_n. \end{aligned} \quad (2)$$

The first term on the right-hand side represents temperature and salinity changes associated with density, that is, dT_ρ . The second term on the right-hand side denotes changes of spiciness. Note that the derivatives with respect to ρ describe the stratification of T and S in the ocean, that is, they are environmental quantities, and are distinct from the thermal and haline expansion coefficients $\alpha = -(\partial\rho/\partial T)|_{T_0, S_0}$, $\beta = (\partial\rho/\partial S)|_{T_0, S_0}$ that are thermodynamic properties of sea water.

Equation (2) also predicts dT_n expected from subduction of surface temperature and salinity anomalies into the thermocline, and will be used to investigate if the surface signals of temperature and salinity are consistent with the changes on isopycnals in the thermocline. Note that, depending on the stability ratio ($\partial T_0/\partial\rho$ and $\partial S_0/\partial\rho$) of the water column, subduction of anomalous warm or salty waters can lead to warm or cool temperature anomalies dT_n on isopycnal surfaces (Church et al. 1991; Bindoff and McDougall 1994; Yeager and Large 2004).

5. Signal detection

Because spiciness anomalies only affect the coupled system when emerging at the surface, the effective forcing of the coupled feedbacks is the surface evolution of χ . The leading empirical orthogonal function (EOF; Fig. 5) of the tracer difference of the WARM and COOL experiments accounts for the majority of the variance (58%, with a spatial loading pattern that is identical to the average). Its principal component captures the arrival of the forced spiciness signal at the surface in the first 2 yr of the experiment and remains approximately constant thereafter. This evolution is approximated by an exponential function

$$F(t) = 1 - \exp[-(t - t_0)/15 \text{ months}]$$

for $t > t_0$, where t_0 corresponds to February of year 100 (Fig. 5). The response of other variables is obtained as the regression of the ensemble mean difference of the WARM and COOL experiments on this exponential function.

The significance of the coupled response is evaluated

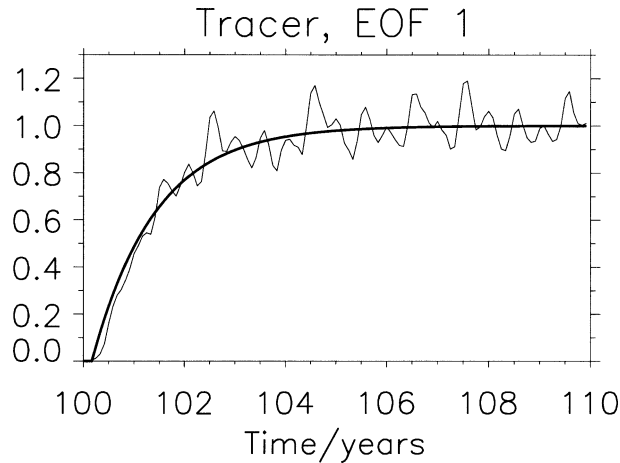


FIG. 5. Principal component of the leading EOF of the spiciness tracer at the surface in the Pacific (from 25°S to 25°N, and from 100°E to 70°W), differenced between the average experiments WARM and COLD. The mode captures 58% of the variance. Superimposed as a heavy line is an exponential fit used to obtain the response of other variables.

using a Student's t test, and degrees of freedom estimated from decorrelation times of 6 months for oceanic and 1.5 months for atmospheric variables, and the variance within the ensembles. The latter is obtained by assuming that the variability within the ensemble does not depend on the spiciness forcing. In the Tropics this is not strictly true. However, results presented are qualitatively robust when this assumption is relaxed, or when the decorrelation times are altered slightly. In light of the few realizations at our disposal, we chose as a significance cutoff 0.1, and allow for a 10% chance that the results presented are due to random fluctuations rather than due to the spiciness forcing. In the following plots, significant signals are marked by shades of gray; insignificant changes are left white.

6. Surface tracer and temperature

The spiciness anomalies are gradually advected and mixed from the equatorial undercurrent to the surface and emerge in a wide swath along the equator from 160°E to 110°W. Surface perturbations are of the order of 0.4 K in the central equatorial Pacific at 150°W (Fig. 6), and dominate the response of tropical surface temperature (Fig. 7). Maximum temperature anomalies and tracer concentrations extend from 5°S to 5°N at the date line, and to 2°N at 130°W. The slight displacement to the south of the equator of the largest temperature and tracer anomalies reflects a similar displacement of the mean equatorial upwelling due to the northward component of the equatorial trades. In the western Pacific, tracer and surface temperature extend in a southeastward direction under the South Pacific convergence zone due to advection by the poleward mean flow.

Compared to the spiciness signal in the thermocline

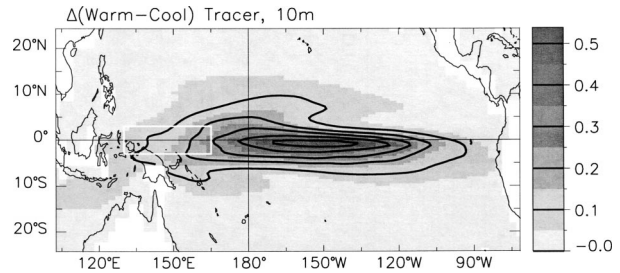


FIG. 6. Difference of tracer (K) between experiments WARM and COLD. Contour level is 0.1 K and is shown in the grayscale on the right. The white box outlines the region of spiciness forcing in the thermocline.

just east of the generation region (Fig. 4), the surface temperature perturbation is much diminished (Fig. 7). After generation, the spiciness anomalies occupy a narrow density and depth range in the thermocline. During their eastward transit the anomalies mix with waters untainted by the spiciness forcing and spread over a larger depth range. The dilution justifies the strong forcing applied to only a fraction of the source waters of equatorial upwelling in the equatorial Pacific, and also indicates that observed spiciness anomalies affect the surface conditions in an appreciable way only if a large fraction of the source waters carry like-signed spiciness anomalies.

7. Heat fluxes

The emergence of a warm spiciness anomaly is associated with venting of heat from the ocean to atmosphere. The anomalous heat flux (Fig. 8) has values of up to 7 W m^{-2} . East of the date line and west of 140°W, the heat fluxes are largest just south of the equator; west of the date line, anomalous fluxes occupy both hemispheres between 5° latitude of the equator.

In the emergence region, the surface flux perturbation is dominated by the latent heat flux with a cooling tendency of up to 9 W m^{-2} . Together with the correlated but smaller sensible heat flux, the turbulent components (Fig. 9) are collocated with the emerging spiciness pattern, suggesting a direct response of the latent and sensible heat fluxes to the changes of SST. The radiative

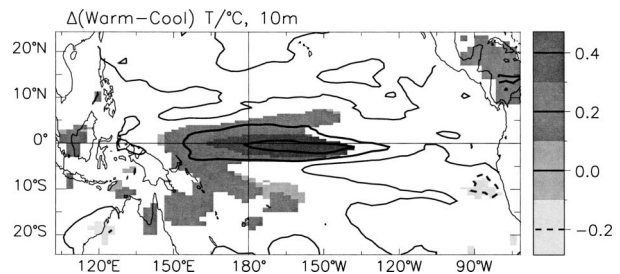


FIG. 7. Difference of SST (K) between experiments WARM and COLD. Differences that are significant at a 0.1 significance level are shown by shades of gray. Contour interval is 0.2 K.

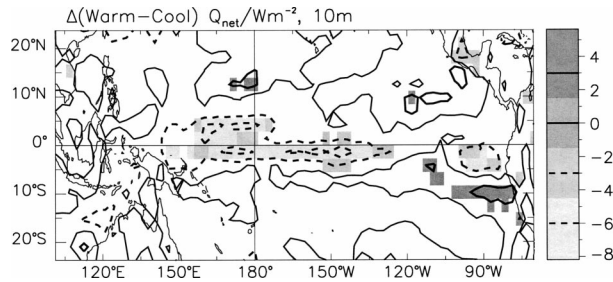


FIG. 8. Same as Fig. 7, but for net heat flux (W m^{-2}), where positive values correspond to an oceanic heat gain. Gray shades show results significant at the 0.1 level. Contour interval is 3 W m^{-2} .

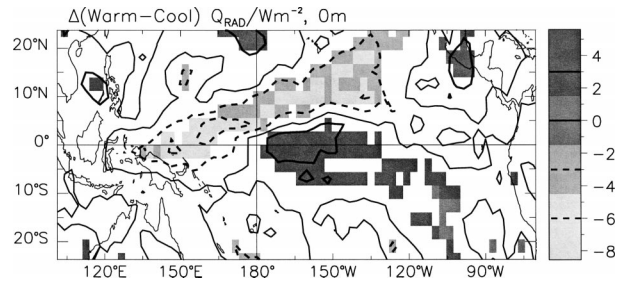


FIG. 10. Same as Fig. 7, but for radiative heat flux, the sum of shortwave and longwave components (W m^{-2}). Positive values correspond to a oceanic heat gain. Gray shades show results significant at the 0.1 level. Contour interval is 3 W m^{-2} .

fluxes (Fig. 10) reflect the shortwave component, which is partially offset by the longwave component. Radiation reduces the turbulent cooling tendency over the emergence region; in the western Pacific, the radiative components dominate the surface heat flux.

The artificial spiciness forcing in the thermocline heats the ocean at a rate of $5.87 \times 10^{13} \text{ W}$, as estimated by integration of the surface flux of tracer over the entire Indo-Pacific. The surface net heat flux (Fig. 8) integrated from 6°S to 6°N , and from 140°E to 120°W , removes $4.337 \times 10^{13} \text{ W}$ primarily by the latent and sensible heat fluxes ($3.60 \times 10^{13} \text{ W}$). The radiative components, integrated over this area, contribute only $0.6 \times 10^{13} \text{ W}$ additional cooling, due to the cancellation of the flux change east and west of the date line. Thus, the majority of the heat added by the forcing is removed locally in the emergence region. The remainder of the heat ($1.55 \times 10^{13} \text{ W}$) is advected out of the equatorial Pacific and leaves the ocean in areas other than the emergence region due to a nonlocal adjustment of the heat budget, or represents heat storage due to internal variability of the ocean–atmosphere system.

8. Freshwater flux, salinity, and wind stress

The spiciness heating enters the atmosphere largely in the form of evaporated water, and is released in the centers of atmospheric deep convection in the western Pacific and intertropical convergence zone. East of the

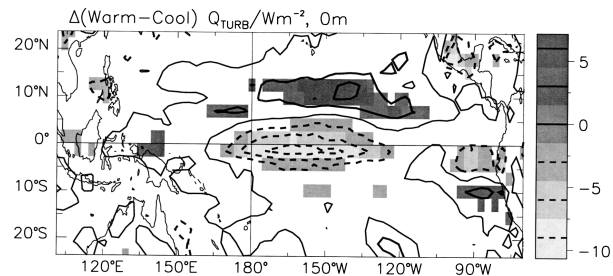


FIG. 9. Same as Fig. 7, but for turbulent heat flux, the sum of latent and sensible fluxes (W m^{-2}). Positive values correspond to an oceanic heat gain. Gray shades show results significant at the 0.1 level. Contour interval is 3 W m^{-2} .

date line and south of 5°N , the freshwater flux (Fig. 11) is dominated by evaporation due to damping of the spiciness heat anomaly with rates of up to 0.3 mm day^{-1} . In the western Pacific and intertropical convergence zone, this latent heat is released in the atmosphere, and precipitation dominates the freshwater flux up to 0.6 to 1.0 mm day^{-1} .

This intensification of the hydrological cycle affects ocean salinity and alters the wind stress. Overall, we note that the freshwater flux cannot remove the salt added by the spiciness forcing—the atmosphere can only redistribute water. Saltier surface waters, thus, prevail, further enhanced by evaporation in the emergence region, and are spread by the mean flow to the west and poleward to a large area with modest spatial gradients (Fig. 12). In the far western Pacific the surface freshwater flux is sufficient to reduce salinity anomalies to small and insignificant values. The only freshening of surface waters occurs in the vicinity of Hawaii, and is associated with increased freshwater flux.

The changes in precipitation and associated atmospheric heating alter the surface wind stress (Fig. 13). On the equator, the zonal wind stress anomalies converge on the date line, with a westward response of up to $4 \times 10^{-3} \text{ N m}^{-2}$ east of the date line, and an eastward wind stress anomalies up to $4 \times 10^{-3} \text{ N m}^{-2}$ and $5 \times 10^{-3} \text{ N m}^{-2}$ in the western Pacific and intertropical convergence zone, respectively. The meridional wind stress response is weaker and of the order of $2 \times 10^{-3} \text{ N m}^{-2}$

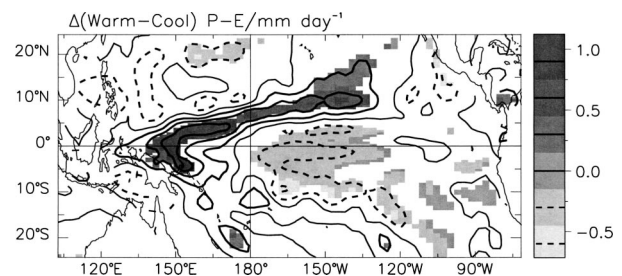


FIG. 11. Same as Fig. 7, but for net freshwater flux (mm day^{-1}). Positive values correspond to a freshening of the ocean. Gray shades show results significant at the 0.1 level. Contour interval is 0.3 mm day^{-1} .

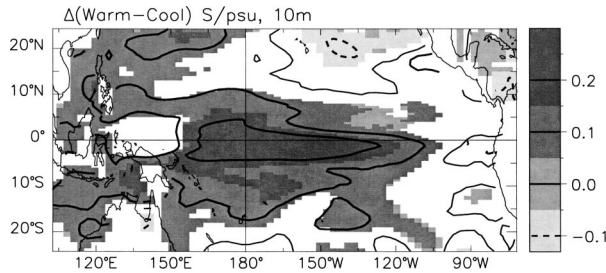


FIG. 12. Same as Fig. 7, but for surface salinity (psu). Gray shading shows results significant at the 0.1 level. Contour interval is 0.1 psu.

with equatorward stress in the western Pacific. East of the date line, northward anomalies prevail from the Southern Hemisphere across the equator to about 10°N. The strong northeastward anomalies at 10°N, 150°W oppose the climatological trade winds, and reduce the winds and cause the positive anomalies of the turbulent heat flux (Fig. 9).

9. Ocean response

The ocean response to these anomalous air–sea fluxes of heat, freshwater, and momentum determines if the emergence of spiciness anomalies can be part of a climate mode. Changes of upper-ocean mixing, isopycnal depth, and spiciness that enhance the surface temperature anomalies in the equatorial region would increase the amplitude of such a mode, and prolong initial disturbances. Spiciness responses upstream from the emergence areas are hypothesized to provide a delayed feedback through changes of extratropical subduction (Gu and Philander 1997), or of speed and path of particles in the thermocline (Schneider 2000). These responses are suggested to be a positive feedback from the Southern Hemisphere (Schneider 2000), and a negative feedback from the Northern Hemisphere (Gu and Philander 1997).

a. Upper-ocean mixing

In the emergence region, the surface buoyancy flux increases vertical mixing in the upper ocean and provides a negative feedback on sea surface temperature. The change in mixing is deduced by comparing responses of ocean currents with wind stress and ocean pressure.

The ocean pressure response is largest at and west of the date line at a depth of 100 m (Fig. 14, top), and results from a deepened thermocline and an increase of pressure by about 50% from values at the surface, due to the increase of density by the surface buoyancy flux. This pressure perturbation accelerates the equatorial zonal currents away from the date line. Together with the wind stress anomalies (Fig. 13) that accelerate the surface waters toward the date line, these forces should

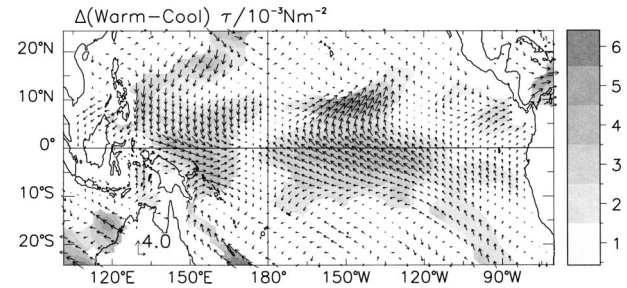


FIG. 13. Same as Fig. 7, but for wind stress in 10^{-3} N m^{-2} . Gray shades show changes of the wind stress magnitude, and are only shown where results are significant at the 0.1 level. Before estimating significance, the wind stress components were rotated to the major axes of variability. Shading interval is 10^{-3} N m^{-2} , the vector scales indicating changes of $4 \times 10^{-3} \text{ N m}^{-2}$ in zonal and meridional directions are depicted over Australia.

increase the vertical shear in the upper ocean. However, the velocity response in the emergence region at and east of the date line is westward, largely insignificant, and without much shear in the upper 100 m (Fig. 14, bottom). This suggests that vertical mixing has increased, as expected, from the surface buoyancy flux. This increased mixing in response to the emergence of warm spiciness anomalies brings cooler thermocline waters to the surface and represents a negative feedback on temperature.

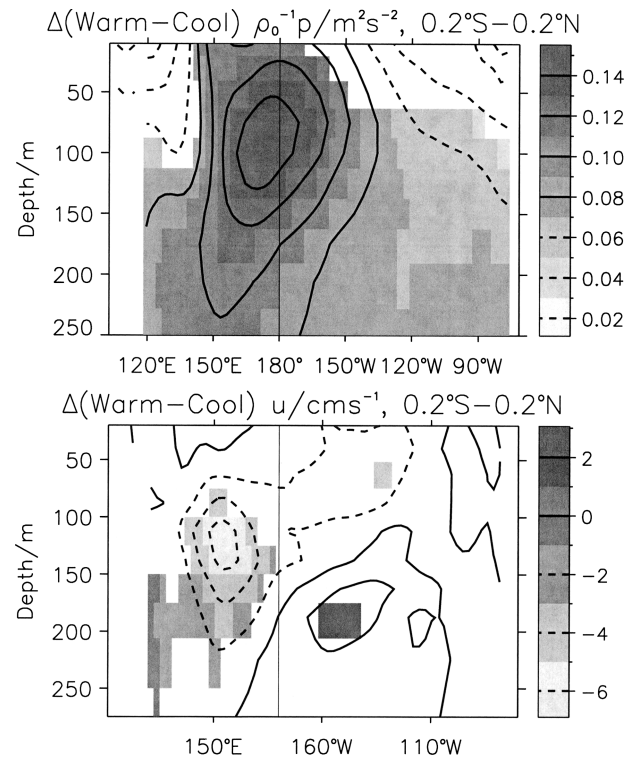


FIG. 14. Changes in (top) oceanic pressure and (bottom) zonal velocity along the equator as a function of longitude and depth. Gray shades denote changes that are significant at the 0.1 level. Contour intervals are $0.02 \text{ m}^2 \text{ s}^{-2}$ and 2 cm s^{-1} , respectively.

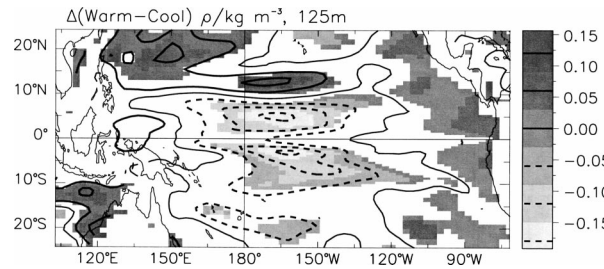


FIG. 15. Same as Fig. 7, but for ocean density at 125 m. Gray shades show results significant at the 0.1 level. Contour interval is 0.06 kg m^{-3} .

b. Ocean density

Oceanic density at 125-m depth decreases in the central Pacific and increases in the east (Fig. 15), consistent with the wind stress response that deepens the equatorial pycnocline in the central Pacific and raises it in the east. Within 10° of the equator, the reduction of density is limited to the central Pacific and is associated with downwelling Ekman pumping. Further west, the downward displacement of the pycnocline is diminished, consistent with the sign reversal of the wind stress curl and Sverdrup dynamics. At the northern flank of the intertropical convergence zone, the wind stress curl lifts the pycnocline, resulting in increases of density at 125-m depths.

Away from the equatorial upwelling region, changes in the depth of the pycnocline are largely independent of changes of SST (Fig. 7). Only off of South America, at 10°S , 85°W , the density response indicates a shallow pycnocline and is associated with cooling at the surface in response to the spiciness forcing (Fig. 7). Off Australia, at 15°S , 160°E , the warm surface temperature anomalies are associated with a strong, local wind stress curl (Fig. 13) and changes of the surface pressure indicating southward advection (not shown).

The deepened pycnocline in the central equatorial Pacific affects the position of the isopycnal outcrops. For the density change of 0.05 kg m^{-3} in a mean east-west gradient of the density of 1 kg m^{-3} (6000 km^{-1}) along the equator, the outcrops move 300 km toward the east. This implies that isopycnals with higher temperatures outcrop further east in response to the emergence of warm spiciness anomalies, a weak positive feedback in the central Pacific.

To quantify the feedback in the equatorial region, the components of the temperature perturbations of Eq. (2) are averaged over the equatorial emergence region. The total temperature response has a subsurface maximum at 120 m in excess of 1 K, largely due to the spiciness forcing (Fig. 16). In the mixed layer above the 80-m depth, dT_ρ is negative and dT_n is positive, and both are of the order of 0.2 K, and reflect the cooling and increase of salinity (and density) due to surface evaporation. In the upper thermocline the deepening of the isopycnals raises temperature dT_ρ by 0.2 K, aided by a weak positive

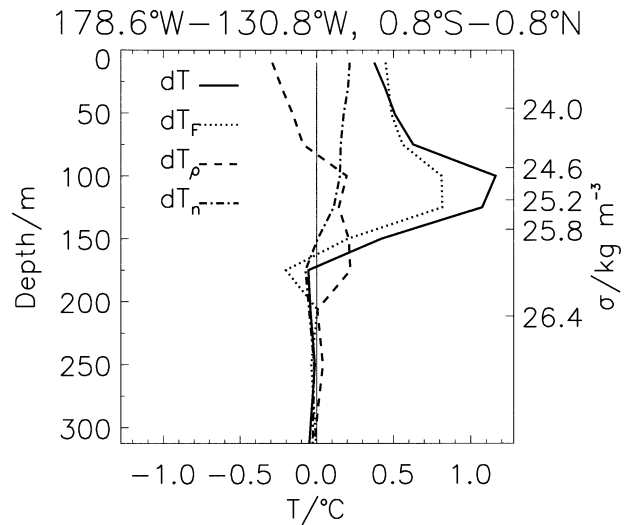


FIG. 16. Change of temperature as a function of depth (m) averaged over the emergence region from 1°S to 1°N , and from 180° to 130°W . Shown are the temperature change (solid line), and its contributions due to the spiciness forcing (dotted, dT_F), due to the feedbacks by changes of density (dashed, dT_ρ) and temperature on isopycnals (dash dot, dT_n). For reference, the mean depth of isopycnals is depicted on the right.

itive dT_n . In all, the response to the spiciness forcing is strongly damped by the air-sea heat flux, and weakly enhanced by the deepening of the thermocline and adjustments of temperature on isopycnals.

c. Spiciness

The response of temperature on isopycnals in the emergence region is part of a large-scale adjustment of spiciness due to altered surface conditions and flow field. After removal of the tracer, the temperature on isopycnals in the thermocline shows that the equatorial region and Southern Hemisphere subtropics are bathed in warm spiciness waters (Fig. 17). South of 10°N , the temperature response on isopycnals is largest right on the equator with values of 0.2 K and results from a northward displacement of the climatological spiciness gradient on the equator, separating salty and warm

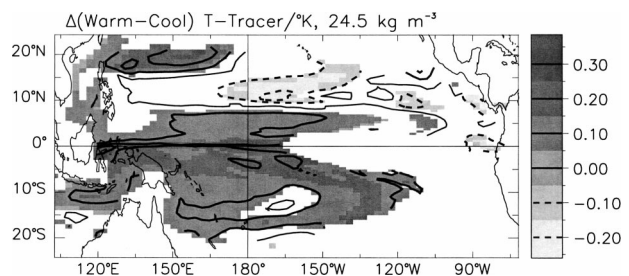


FIG. 17. Same as Fig. 7, but for temperature on the $24.5\text{-}\sigma_\theta$ isopycnal surface. Gray shades show results significant at the 0.1 level. Contour interval is 0.1 K. Uncontoured regions denote areas where the isopycnal surface outcrops or is nonexistent.

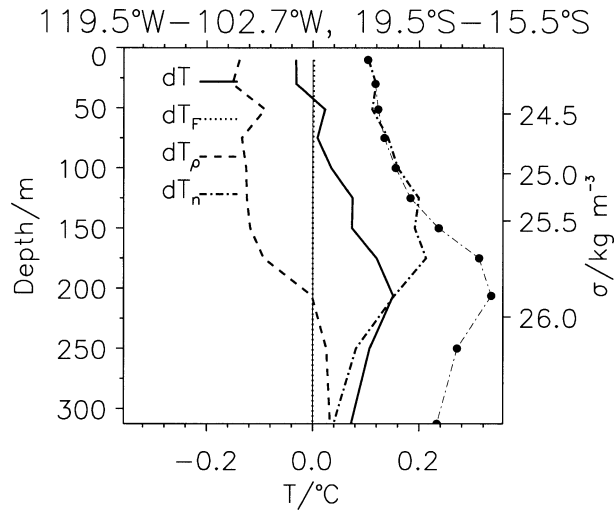


FIG. 18. Change of temperature as a function of depth (m) averaged over the subduction region from 20° to 15° S, and from 120° to 100° W. Shown are the temperature change (solid line), and its contributions due to the spiciness forcing (dotted, dT_F), due to the feedbacks by changes of density (dashed, dT_{ρ}) and temperature on isopycnals (dash dot, dT_n). The temperature changes expected from inserting surface temperature and salinity changes at each depth level are shown by the dash-dot line with filled circles, and represent the simplest model for anomalies of temperature on isopycnals caused by the subduction of surface temperature and salinity anomalies. For reference, the mean depth of isopycnals is depicted on the right.

Southern Hemisphere waters from cool and fresh waters of the Northern Hemisphere (Fig. 2). In addition, the tropical temperature on isopycnals reflects mixing in the shallow equatorial cell that recycles water into the upper-thermocline waters, with increased salinities due to the spiciness forcing and Southern Hemisphere subduction.

In the Southern Hemisphere subduction zone off South America, the surface temperature response is small (Fig. 7), and on-isopycnal perturbations result from changes of surface salinity (Fig. 12). The temperature component dT_{ρ} cools above 200-m depths, and is smaller than the warming by dT_n , which reaches 0.2 K at 150-m depths (Fig. 18). The surface perturbations account for the changes above this isopycnal very well, consistent with the hypothesis of subduction. Below the fit deteriorates, because the local surface temperature and salinity are not representative of conditions at the outcrops of deeper isopycnals.

In the Northern Hemisphere subtropics between 10° and 20° N, cool spiciness anomalies of 0.2 K are generated and emanate from outcrops close to Hawaii in a southwestward and then westward direction (Fig. 17). In this source region, the surface temperature perturbation is close to zero (Fig. 7), while surface salinity is reduced significantly (Fig. 12). The split of temperatures into its components (Fig. 19) shows that dT_{ρ} warms by 0.1 K in the mixed layer, and by 0.2 K in the upper thermocline, while below 120 m dT_{ρ} is reduced by 0.1 K due to shallower isopycnals. Temperatures on iso-

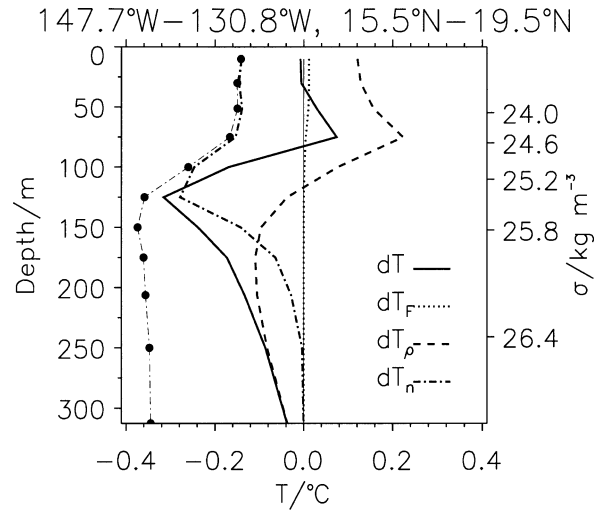


FIG. 19. Same as Fig. 18, but for the Northern Hemisphere subduction region off of Hawaii from 15° to 20° N, and from 150° to 130° W.

pycnals, dT_n , decrease in the upper 250 m, with the largest cooling of 0.3 K at $25.5\sigma_T$ at a depth of 120 m (Fig. 19). Estimating the dT_n from the local surface perturbation of temperature and salinity yields a very good fit for isopycnals shallower than 25.5σ and indicates that subduction of the surface anomalies are consistent with changes on isopycnals in the upper thermocline. For deeper isopycnals, the fit deteriorates because their outcrops are subject to different surface temperature and salinity perturbations.

d. Anomalous advection

In areas of a mean temperature gradient along isopycnals, spiciness anomalies can be generated or diminished by changes of the path of waters, that is, by anomalous advection. This process is evaluated by the Montgomery streamfunction, relative to the value at the equatorial emergence region. Its changes are most prominent in the Northern Hemisphere, with a low extending across the Pacific from 10° to 20° N, in the North Equatorial Current (Fig. 20). This corresponds to an anomalous westward flow of 1 cm s^{-1} on the northern flank, and an eastward flow of 2 cm s^{-1} on the southern flank, which is an increase in the North Equatorial Current and an northward shift of the North Equatorial Countercurrent.

This perturbation of the Montgomery streamfunction is embedded in a mean streamfunction (Fig. 1) that increases in a north-northwestward direction, and implies that streamlines connecting the equatorial emergence and midlatitude subduction regions are displaced to the northwest in the North Equatorial Current, toward higher temperatures on the isopycnal (Fig. 2). The displacement that results from a response of $0.1 \text{ m}^2 \text{ s}^{-2}$ in a mean streamfunction gradient of $4 \text{ m}^2 \text{ s}^{-2} (1000 \text{ km})^{-1}$

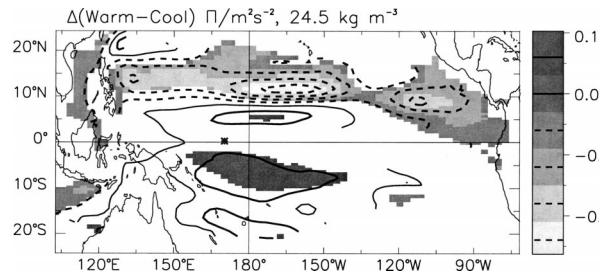


FIG. 20. Same as Fig. 7, but for Montgomery streamfunction on the $24.5\text{-}\sigma_{\theta}$ isopycnal surface. Gray shades show results significant at the 0.1 level. Contour interval is $0.06\text{ m}^2\text{ s}^{-2}$. Uncontoured regions denote areas where the isopycnal surface outcrops or is nonexistent. The sign of the streamfunction implies that on the Northern (Southern) Hemisphere the flow proceeds with a high on its right (left). The streamfunction has been referenced to 170°E on the equator (star symbol), to indicate changes of trajectories of water parcels that enter the equatorial undercurrent in the western Pacific.

is only a very modest few tens of kilometers, and corresponds to cool temperature anomalies of one-tenth of a kelvin given the mean temperature gradient on the isopycnal (Fig. 2). While small, this cooling of isopycnals nevertheless adds to the negative feedback from the subduction region east of Hawaii, and is consistent with an increase of the cool temperature response east of 12°N , 180°W (Fig. 17).

10. Interannual variability

To investigate the dependence of the model's ENSO on the spiciness forcing, the leading EOF of temperature anomalies in the tropics are determined separately for experiments WARM and COOL. The spatial patterns of the leading mode are virtually identical, but the principal components of experiment COOL have a larger amplitude, explain a larger fraction of the total variance, and have a hint of a longer period, than results of experiment WARM (Fig. 21). Averaged from 2°S to 2°N , and from 160° to 110°W , the standard deviation of temperature (based on the EOF reconstruction) is 1.23 K for experiment COOL, compared to 0.9 K for experiment WARM, a difference marginally significant at the 0.1 level.

The spiciness anomalies affect the model's ENSO via control of the strength of the thermocline feedback. In response to a change of the wind stress, the rate of cooling (warming) of the surface mixed layer due to shallowing (deepening) of isopycnals depends on the temperature gradient in density coordinates—the spiciness forcing. Formally, temperature anomalies dT at the base of the surface layer result from vertical undulations of isopycnals and the associated density anomaly $d\rho$, and the stratification of temperature T with density $\partial T_0/\partial\rho$,

$$dT = \frac{\partial T_0}{\partial \rho} d\rho. \quad (3)$$

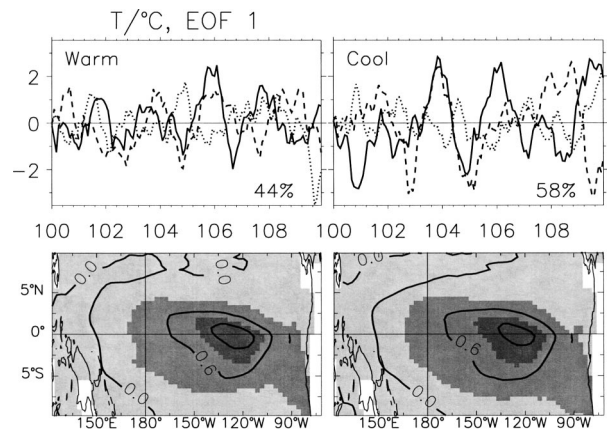


FIG. 21. Leading EOF of anomalies of SST in the tropical Pacific for the (left) WARM and (right) COOL experiments that account for 44% and 58% of the variance of SST, respectively. Before estimation of the EOF, SSTs were smoothed with a 5-month filter with linearly varying weight, and a linear trend was removed. The top panel shows the leading principal component as a function of model year for the three ensemble members (solid, dashed, and dotted lines). Results have been scaled such that the principal component corresponding to the associated temperature variability (K) averaged from 160° to 110°W within 2° of the equator. The bottom panel shows the spatial-loading pattern.

The regression of anomalies of temperature and density, a measure for $\partial T_0/\partial\rho$, reveals that on the western flank of the ENSO signal, the decrease of temperature with increasing density is larger for experiment COOL compared to experiment WARM (Fig. 22). Further, east and west of this region no significant changes are found.

This difference of $\partial T_0/\partial\rho$ implies that a westward (eastward) wind stress result in a cooling (warming) tendency of the surface mixed layer that is larger in experiment COOL compared to WARM. The feedback with the winds is, therefore, increased in experiment COOL consistent with the larger amplitude of ENSO. One hypothetical extreme case of experiment WARM, mentioned in the introduction, is an isothermal equatorial ocean with a strong salinity stratification. In this case, the thermocline feedback is absent, because undulations of the pycnocline do not affect surface temperature, and ENSO should not exist.

11. Midlatitude response

Considering the changes in tropical precipitation in response to the emergence of the spiciness anomalies, it comes as no surprise that the midlatitude oceans are affected via atmospheric teleconnections. Sea surface temperatures show a large response; in fact the largest feedback outside of the emergence area is in the Kuroshio–Oyashio Extension region (Fig. 23). The SST signals coincide with change of the circulation, as measured by sea level (Fig. 24), and changes of Ekman pumping over the North Pacific. This suggests that in response to equatorial emergence of warm spiciness

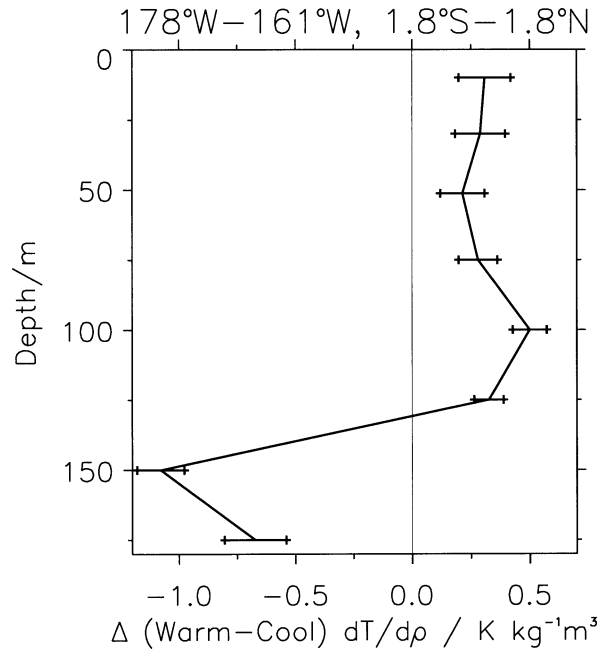


FIG. 22. Difference of regression between interannual anomalies of temperature and density between the WARM and COOL experiments, as a function of depth, with 90% confidence interval noted by horizontal lines. Note that temperature decreases with increasing density; thus, a positive difference implies that the change of temperature with density is stonger for experiment COOL.

anomalies, the boundary between subtropical and subpolar North Pacific gyres shift equatorward, leading to cool SSTs off of Japan. This process is reminiscent of the generation of decadal North Pacific temperature variations (Miller et al. 1998; Seager et al. 2001; Schneider et al. 2002).

12. Discussion and conclusions

The adjustment of the coupled ocean-atmosphere system to the equatorial emergence of density-compensated temperature and salinity, or spiciness, anomalies is studied. This adjustment is of interest because of its possible role in decadal modulation of climate, where spiciness anomalies in the thermocline are advected as a passive tracer to the equatorial upwelling region, and, upon emerging at the equator, alter the surface heat budget and interact with the atmosphere.

The emergence of warm and salty spiciness anomalies at the surface is marked by warm SSTs and high sea surface salinity (SSS) anomalies in the central equatorial Pacific, a removal of most of the heat anomaly by the latent heat flux, and an increase of vertical mixing. The excess moisture entering the atmosphere enhances precipitation in the intertropical convergence zone and enhances southeasterly trade winds at, and east of, the date line, and northerly winds east of the date line and north of the equator. In the west Pacific, eastward wind stress anomalies result.

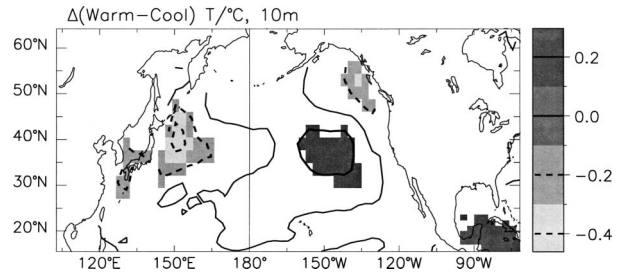


FIG. 23. Same as Fig. 7, but for sea surface temperature in the North Pacific. Gray shades show results are significant at the 0.1 level. Contour interval is 0.2 K.

The changes in the wind stress depress the low-latitude pycnocline and, thereby, enhance the surface temperature anomalies via the thermocline feedback. An additional weak, positive feedback derives from the northward displacement of the climatological spiciness front on the equator, Southern Hemisphere subduction, and recycling of surface salinity anomalies due to the forcing. In contrast, in the Northern Hemisphere subtropics off of Hawaii, fresh and cool anomalies are created by freshening of the surface layer and are further strengthened by anomalous advection during transit to the western boundary. Thus, the Northern Hemisphere response represents a negative, delayed feedback to the spiciness forcing.

The coupled response is qualitatively consistent with a climate mode that results from a positive feedback between the equatorial emergence of spiciness anomalies and the equatorial pycnocline and Southern Hemisphere response, and a delayed, negative feedback due to Northern Hemisphere subduction (Gu and Philander 1997; Schneider 2000; Giese et al. 2002). However, the overall feedback on surface temperature in the equatorial region is negative due to vertical mixing, inconsistent with Giese et al. (2002), and the extratropical feedback is weak and occurs at lower latitudes than in Gu and Philander (1997). For a spiciness anomaly of 1 K in the equatorial pycnocline, the surface perturbation of the order of 0.5 K, the subducted anomalies on the Northern Hemisphere are of the order of 0.2–0.3 K. Thus, at most, the feedbacks slightly enhance a decadal

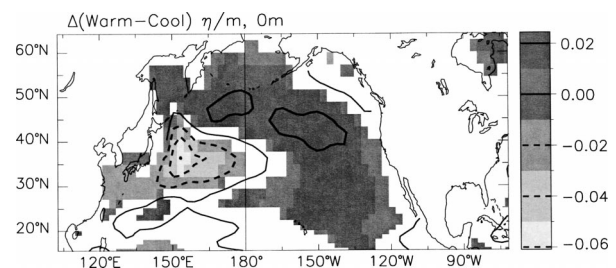


FIG. 24. Same as Fig. 7, but for surface elevation in the North Pacific. Gray shades show results are significant at the 0.1 level. Contour interval is 0.02 m.

modulation of the Tropics due to spiciness anomalies generated by stochastic atmospheric forcing.

In addition to the tropical feedbacks, spiciness anomalies in the eastern equatorial upwelling region affect the midlatitude North Pacific. The changes in centers of deep convection in the tropical atmosphere are teleconnected to the northern midlatitudes during boreal winter. In the North Pacific, the westerly wind regime is shifted to the south and leads to a cyclonic anomalous circulation, including a southward shift of the Kuroshio–Oyashio current system. This leads to cool anomalies off of Japan, the largest surface temperature response to the emerging spiciness anomalies at the equator.

The amplitude of the model's ENSO is smaller for warm spiciness anomalies in the equatorial thermocline. This occurs due to a reduction of the thermocline feedback by an upper-ocean decrease of temperature gradient in density coordinates. In models of ENSO, the thermocline feedback is included by a parameterization of the temperature at the base of the equatorial mixed layer in terms of the depth of thermocline (Seager et al. 1988). Spiciness anomalies affect this relation, and, thus, should be included in studies of the sensitivity of ENSO to the background state (e.g., Fedorov and Philander 2001).

These results have to be viewed in light of specifics of the experimental setup. The spiciness anomalies were introduced into the model in the upper thermocline in the western Pacific. The gradual upward mixing and appearance of the spiciness anomalies over a large part of the upwelling region indicates that the results are insensitive to modest changes of the isopycnal location of the forcing. However, spiciness anomalies on deeper isopycnals would likely emerge further east. This should enhance the area of eastward equatorial winds west of the emergence region, at the expense of the westward winds to its east. We do not expect this to change the downward displacement of isopycnals in the emergence region, nor the feedback due to the thermocline feedback.

A more serious problem in using these results are model deficiencies: the equatorial cold tongue extends too far westward, and the intertropical convergence zone, while good compared to many other coupled model simulations, is too symmetric about the equator. In addition, the resolution of the model does not allow for vigorous equatorial currents, and might discriminate against advective processes and emphasize the thermocline feedback. Other models, preferably with increased resolution should be employed to estimate the robustness of the results presented here.

The application of these numerical results to explain observed, low-frequency variations in the equatorial Pacific is inconclusive. Long time series of temperature and salinity in the upper subtropical and tropical Pacific exist close to the island of Oahu (Lukas 2001), and along 137° (Suga et al. 2000) and 165°E (Kessler 1999). Observed low-frequency changes of salinity or temperature

(or salinity) on isopycnals are of the order of 0.5 K, comparable in magnitude to the forcing used in the model. However, it is unclear if the observed anomalies are representative of spiciness anomalies that emerge in the downstream eastern equatorial upwelling region.

In the model, large spiciness anomalies are generated in a small area in the western Pacific and are reduced to realistic magnitude by mixing with source waters of the Equatorial Undercurrent untainted by the spiciness forcing. This implies that observed spiciness anomalies have to occupy simultaneously a large fraction of the source waters of equatorial upwelling. This could result either from coherent forcing or be a chance occurrence due to the mixing of spiciness anomalies generated by stochastic atmospheric forcing (Hall and Manabe 1997). In the latter case, the low-frequency variability in the Tropics would reflect the stochastic perturbations in the off-equatorial subduction region and along the thermocline path of both hemispheres.

The results presented here show that the two-component nature of sea water is important to the coupled evolution of the tropical climate. To determine if the simulated processes do indeed account for a fraction of the observed decadal variability in the Tropics requires first of all of the long time series of temperature and salinity in the upper tropical Pacific. Such observations are now beginning to be collected in the Tropical Ocean and Global Atmosphere (TOGA) Tropical Atmosphere–Ocean (TAO) array and as part of the ARGO project.

Acknowledgments. The author thanks Drs. Bruce Cornuelle, Arthur J. Miller, David W. Pierce, and Jim Potemra for helpful discussions and comments on the manuscript. This paper is funded by the National Science Foundation (OCE00-82543) and the Department of Energy (DE-FG03-01ER63255). The views expressed herein are those of the author and do not necessarily reflect the views of NSF or DOE or any of their sub-agencies.

REFERENCES

- Bindoff, N. L., and T. J. McDougall, 1994: Diagnosing climate change and ocean ventilation using hydrographic data. *J. Phys. Oceanogr.*, **24**, 1137–1152.
- Church, J. A., J. S. Godfrey, D. R. Jackett, and T. J. McDougall, 1991: A model of sea level rise caused by ocean thermal expansion. *J. Climate*, **4**, 438–456.
- Fedorov, A. V., and S. G. Philander, 2001: A stability analysis of tropical ocean–atmosphere interactions: Bridging measurements and theory for El Niño. *J. Climate*, **14**, 3086–3101.
- Frey, H., M. Latif, and T. Stockdale, 1997: The coupled model ECHO-2. Part I: The tropical Pacific. *Mon. Wea. Rev.*, **125**, 703–720.
- Giese, B. S., S. C. Urizar, and N. S. Fuckar, 2002: Southern Hemisphere origins of the 1976 climate shift. *Geophys. Res. Lett.*, **29**, 1014, doi:10.1029/2001GL013268.
- Gordon, A. L., 1986: Interocean exchange of thermocline water. *J. Geophys. Res.*, **91C**, 5037–5050.
- Gu, D. F., and S. G. H. Philander, 1997: Interdecadal climate fluctuations that depend on exchanges between the Tropics and extratropics. *Science*, **275**, 805–807.

- Hall, A., and S. Manabe, 1997: Can local linear stochastic theory explain sea surface temperature and salinity variability? *Climate Dyn.*, **13**, 167–180.
- Johnson, G. C., and M. J. McPhaden, 1999: Interior pycnocline flow from the subtropical to the equatorial Pacific Ocean. *J. Phys. Oceanogr.*, **29**, 3073–3089.
- Kessler, W. S., 1999: Interannual variability of the subsurface high salinity tongue south of the equator at 165°E. *J. Phys. Oceanogr.*, **29**, 2038–2049.
- Kleeman, R., J. P. McCreary, and B. A. Klinger, 1999: A mechanism for generating ENSO decadal variability. *Geophys. Res. Lett.*, **26**, 1743–1746.
- Latif, M., and T. P. Barnett, 1994: Causes of decadal climate variability over the North Pacific and North America. *Science*, **266**, 634–637.
- Lukas, R., 2001: Freshening of the upper thermocline in the North Pacific subtropical gyre associated with decadal changes of rainfall. *Geophys. Res. Lett.*, **28**, 3485–3488.
- , and E. Lindstrom, 1991: The mixed layer of the western equatorial Pacific. *J. Geophys. Res.*, **96** (Suppl.), 3343–3357.
- McCreary, J. P., and P. Lu, 1994: Interaction between the subtropical and equatorial ocean circulation—The subtropical cell. *J. Phys. Oceanogr.*, **24**, 466–497.
- Miller, A. J., D. R. Cayan, and W. B. White, 1998: A westward intensified decadal change in the North Pacific thermocline and gyre-scale circulation. *J. Climate*, **11**, 3112–3127.
- Munk, W., 1981: Internal waves and small scale processes. *Evolution of Physical Oceanography*, B. A. Warren and C. Wunsch, Eds., MIT Press, 264–291.
- Pierce, D. W., T. P. Barnett, and M. Latif, 2000: Connections between the Pacific Ocean Tropics and midlatitudes on decadal time scales. *J. Climate*, **13**, 1173–1194.
- Roeckner, E., and Coauthors, 1996: The atmospheric general circulation model ECHAM-4: Model description and simulation of present-day climate. Max-Planck-Institute for Meteorology Tech. Rep. 218, 99 pp. [Available from DKRZ, Bundesstr. 55, 20146 Hamburg, Germany.]
- Schneider, N., 2000: A decadal spiciness mode in the Tropics. *Geophys. Res. Lett.*, **27**, 257–260.
- , A. J. Miller, and D. W. Pierce, 2002: Anatomy of North Pacific decadal variability. *J. Climate*, **15**, 586–605.
- Seager, R., S. E. Zebiak, and M. A. Cane, 1988: A model of the tropical Pacific sea surface temperature climatology. *J. Geophys. Res.*, **93**, 1265–1280.
- , Y. Kushnir, N. Naik, M. A. Cane, and J. A. Miller, 2001: Wind-driven shifts of the Kuroshio–Oyashio Extension and the generation of SST anomalies on decadal time scales. *J. Climate*, **14**, 4249–4265.
- Suga, T., A. Kato, and K. Hanawa, 2000: North Pacific tropical water: Its climatology and temporal changes associated with the climate regime shift in the 1970s. *Progress in Oceanography*, Vol. 47. Pergamon, 223–256.
- Yeager, S. G., and W. G. Large, 2004: Late winter generation of spiciness on subducted isopycnals. *J. Phys. Oceanogr.*, in press.